## Eye-dominance-guided Foveated Rendering

Xiaoxu Meng, Ruofei Du, and Amitabh Varshney, Fellow, IEEE

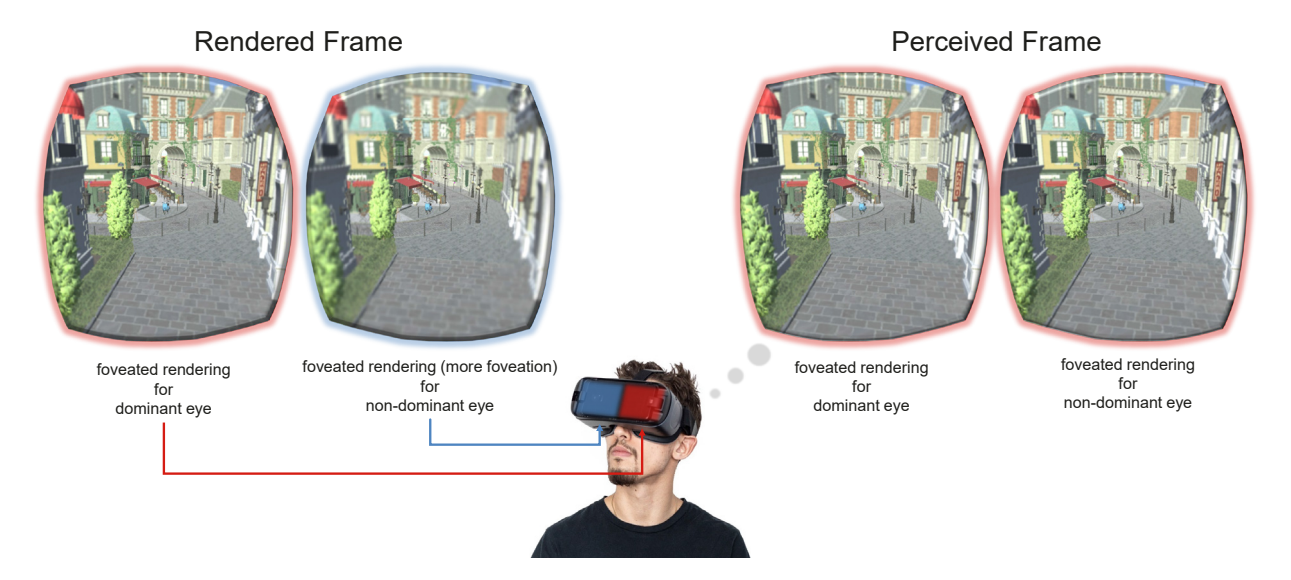


Fig. 1. Our pipeline renders the frames displayed in the dominant eye at a lower foveation level (with higher detail), and renders the frames for the non-dominant eye at a higher foveation level. This improves rendering performance over traditional foveated rendering with minimal perceptual difference.

Abstract— Optimizing rendering performance is critical for a wide variety of virtual reality (VR) applications. Foveated rendering is emerging as an indispensable technique for reconciling interactive frame rates with ever-higher head-mounted display resolutions. Here, we present a simple yet effective technique for further reducing the cost of foveated rendering by leveraging ocular dominance — the tendency of the human visual system to prefer scene perception from one eye over the other. Our new approach, eye-dominance-guided foveated rendering (EFR), renders the scene at a lower foveation level (with higher detail) for the dominant eye than the non-dominant eye. Compared with traditional foveated rendering, EFR can be expected to provide superior rendering performance while preserving the same level of perceived visual quality.

Index Terms—Virtual reality, foveated rendering, perception, gaze-contingent rendering, ocular dominance, eye tracking

## 1 Introduction

Foveated rendering [11,24,33] aims to improve the rendering efficiency while maintaining visual quality by leveraging the capabilities and the limitations of the human visual system. Equipped with an eyetracker, a foveated rendering system presents the foveal vision with full-resolution rendering and the peripheral vision with low-resolution rendering. This allows one to improve the overall rendering performance while maintaining high visual fidelity.

The human visual system has a tendency to prefer visual stimuli of one eye more than the other eye [29]. This phenomenon is referred to as eye (or ocular) dominance. The dominant eye is found to be superior to the non-dominant eye in visual acuity, contrast sensitivity [32], color discrimination [17], and motor functions that are visually managed and require spatial attention [23].

In this paper, we propose the technique of eye-dominance-guided foveated rendering (EFR), which leverages ocular dominance property of the human visual system. We render the scene for the dominant eye

- Xiaoxu Meng is with University of Maryland, College Park. E-mail: xmeng525@umiacs.umd.edu.
- Ruofei Du is with Google LLC. E-mail: ruofei@google.com.
- Amitabh Varshney is with University of Maryland, College Park. E-mail: varshney@umiacs.umd.edu.

Manuscript received 10 Sept. 2019; accepted 5 Feb. 2020. Date of publication 18 Feb. 2020; date of current version 27 Mar. 2020. Digital Object Identifier no. 10.1109/TVCG.2020.2973442 at the normal foveation level and render the scene for the non-dominant eye at a higher foveation level. This formulation allows us to save more in the rendering budget for the non-dominant eye. We have validated our approach by carrying out quantitative experiments and user studies. Our contributions include:

- designing eye-dominance-guided foveated rendering, an optimized technique for foveated rendering, that provides similar visual results as the original foveated rendering, but at a higher rendering frame rate;
- conducting user studies to identify the parameters for the dominant eye and the non-dominant eye to maximize perceptual realism and minimize computation for foveated rendering in headmounted displays; and,
- 3. implementing the eye-dominance-guided foveated rendering pipeline on a GPU, and achieving up to  $1.47 \times$  speedup compared with the original foveated rendering at a resolution of  $1280 \times 1440$  per eye with minimal perceptual loss of detail.

The rest of the paper is organized as follows: Section 2 summarizes the development of foveated rendering as well as ocular dominance. Our algorithm of eye-dominance-guided foveated rendering technique and its implementation follow in Section 3. The user study experiments are introduced in Section 4. Results of the user study and the perfor-

mance evaluation are presented in Section 5. We conclude the paper and propose future directions in Section 6.

## 2 RELATED WORK

Rendering speed and transmission bandwidth are two critical constraints in realizing effective and distributed virtual reality [6]. In this section, we review the relevant state-of-the-art research in foveated rendering and eye-dominance that inspires our work.

## 2.1 Foveated Rendering

As reviewed by Weier et al. [41], foveated rendering for 3D geometries includes perception-based mesh simplification in the lower acuity areas [13, 14, 25] and low-level mesh-feature extraction with a saliency map [19, 43]. It is crucial to achieve high rendering efficiency for modern VR applications. He et al. [12] and Vaidyanathan et al. [40] implement rendering systems with coarse-pixel to achieve interactive frame rates. Ragan-Kelley et al. [30] propose decoupled sampling, which leverages stochastic super-sampling of motion and defocus blur to reduce the shading cost. Guenter et al. [11] couple foveated rendering with eye-tracking and present the seminal foveated rendering pipeline with three eccentricity layers around the tracked gaze point. Vaidyanathan et al. [40] and Patney et al. [28] perform foveated rendering by sampling coarse pixels in the peripheral regions. Clarberg et al. [5] propose adaptive multi-frequency shading to support flexible control of the shading rates and automatic shading reuse between triangles in tessellated primitives. He et al. [12] introduce multi-rate GPU shading, which enables more shading samples near regions of specular highlights, shadows, edges, and motion blur regions. Bektas et al. [1] present a testbed featuring gaze-contingent displays, which can manage the visual level of detail. With multiple models of the human visual system combined, the system can respond to the viewer's gaze in real-time and render a space-variant visualization. Swafford et al. [37] summarize four foveated rendering methods: the first one reduces peripheral resolution; the second one varies per-pixel depth-buffer samples in the fovea and periphery for screen-space ambient occlusion; the third one implements a terrain renderer using GPU-level tessellation for the fovea, and the last one varies the per-pixel ray-casting steps across the field of view. Stengel et al. [33] use adaptive sampling from fovea to peripheral regions in a gaze-contingent deferred shading pipeline.

Meng et al. [24] present kernel foveated rendering (KFR), which parameterizes foveated rendering by embedding polynomial kernel functions in the classic log-polar mapping, thus allowing users to vary the sampling density and distribution that matches human perception. Turson et al. [39] study the resolution requirements at different eccentricities as a function of luminance patterns and derive a low-cost predictor of the foveated rendering parameters. The lower level of detail in peripheral regions in foveated rendering may cause spatial and temporal artifacts. Patney et al. [28] enhance the image quality of foveated rendering [40] by temporal anti-aliasing and contrast preservation. Turner et al. [38] propose an algorithm to reduce motion artifacts in the periphery of foveated rendering by aligning the rendered pixel grid to the virtual scene content during rasterization and upsampling.

Foveated rendering is also playing a significant role in video streaming. Lungaro *et al.* [10,21] propose to use a tile-based foveated rendering algorithm to reduce the overall bandwidth requirements for streaming 360° videos. Kaplanyan *et al.* present *DeepFovea* [15], which uses generative adversarial neural networks to reconstruct a plausible peripheral video from a small fraction of pixels provided every frame.

Besides virtual reality, foveated rendering is also desirable for augmented reality [16] and light field displays [35].

## 2.2 Eye Dominance

Eye dominance has been described as the inherent tendency of the human visual system to prefer scene perception from one eye over the other [29]. Einat and Shaul [32] study the role of eye dominance in dichoptic visual search by comparing performance with target presented to the dominant or the non-dominant eye. They conclude that the dominant eye has priority in visual processing, perhaps even resulting in inhibition of non-dominant eye representations. Oishi *et al.* [26]

observe that the dominant eye is functionally activated prior to the non-dominant eye in conjugate eye movements. Koctekin *et al.* [17] find that the dominant eye has priority in red/green color spectral region, leading to better color-vision discrimination ability. Chaumillon *et al.* [3] show that sighting eye dominance has an influence on visually triggered manual action with shorter reaction time.

In this work, we take advantage of the weaker sensitivity and acuity of the non-dominant eye and render the non-dominant display with greater foveation to overall accelerate foveated rendering.

## 3 OUR APPROACH

Here we present an overview of the parameterized foveated rendering and then we build upon it to accomplish eye-dominance-guided foveated rendering.

## 3.1 Foveation Model

We use the kernel foveated rendering (KFR) model [24] because this model parameterizes the level of foveation with two simple parameters: frame buffer parameter  $\sigma$  controls the width of the frame-buffer to be rendered, thus controlling the level of foveation; and the kernel function parameter  $\alpha$  controls the distribution of pixels.

The KFR model contains two passes. In the first pass, the renderer transforms the shading materials in the G-buffer (world positions, texture coordinates, normal maps, albedo maps, etc.) from the Cartesian coordinates to kernel log-polar coordinates. Because of the non-uniform scaling effect in the transformation, details in the foveal region are preserved and details in the peripheral region are reduced.

Given a screen of resolution  $W \times H$ , for each pixel coordinate (x, y) with foveal coordinate  $\mathbf{F}(\mathring{x}, \mathring{y})$ , we define (x', y') as

$$x' = x - \mathring{x},$$
  

$$y' = y - \mathring{y}.$$
(1)

Then, KFR transforms the point (x', y') to (u, v) in the kernel logpolar space via Equation 2:

$$u = \frac{1}{\sigma} \left( \frac{\log \left\| \frac{W}{2} x', \frac{H}{2} y' \right\|_{2}}{L} \right)^{-\alpha},$$

$$v = \frac{1}{\sigma} \left( \arctan \left( \frac{y'}{x'} \right) \frac{1}{2\pi} + \mathbf{1} \left[ y' < 0 \right] \right),$$
(2)

where L is the log of the maximum distance from  $\mathbf{F}(\mathring{x},\mathring{y})$  to the farthest screen corner as shown in Equation 3:

$$L = \log(\max(\max(l_1, l_2), \max(l_3, l_4))). \tag{3}$$

Here,

$$l_{1} = \sqrt{\mathring{x}^{2} + \mathring{y}^{2}},$$

$$l_{2} = \sqrt{(W - \mathring{x})^{2} + (H - \mathring{y})^{2}},$$

$$l_{3} = \sqrt{\mathring{x}^{2} + (H - \mathring{y})^{2}},$$

$$l_{4} = \sqrt{(W - \mathring{x})^{2} + \mathring{y}^{2}}.$$
(4)

In the second pass, the renderer transforms the rendered scene from kernel log-polar coordinates to Cartesian coordinates and renders to the full-resolution screen. A pixel with log-polar coordinates (u,v) is transformed back to (x'',y'') in Cartesian coordinates as shown in Equation 5:

$$x'' = \exp(L \cdot (u\sigma)^{\alpha})\cos(2\pi \nu) + \mathring{x},$$
  

$$y'' = \exp(L \cdot (u\sigma)^{\alpha})\sin(2\pi \nu) + \mathring{y}.$$
(5)

According to [24], the kernel function parameter is suggested as  $\alpha=4$ . Therefore, we can control the level of foveation by only altering the parameter  $\sigma$ .

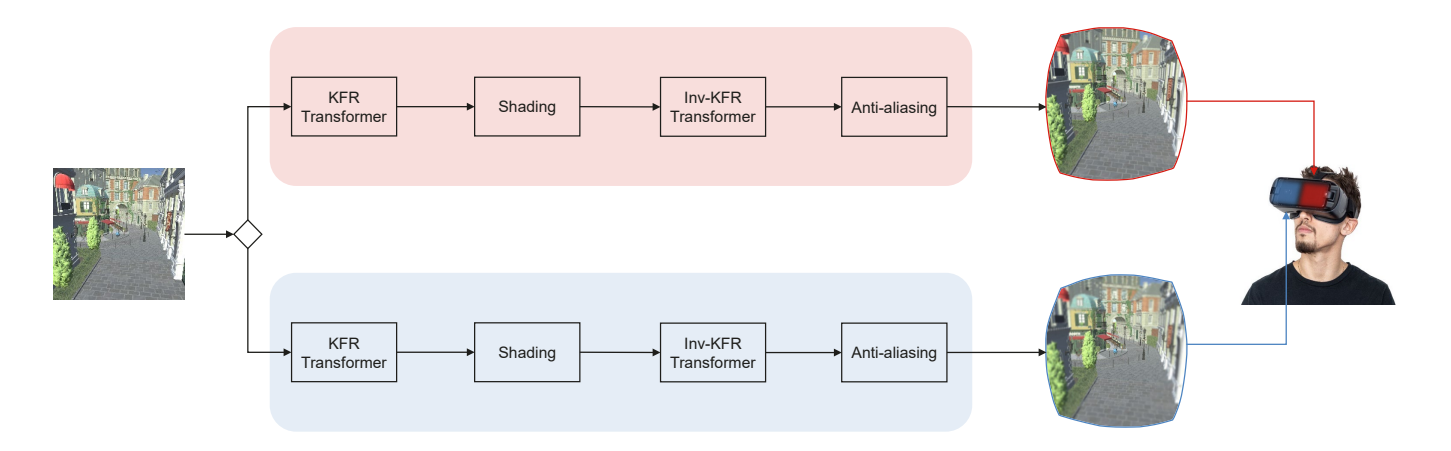


Fig. 2. An overview of the eye-dominance-guided foveated rendering system. Our system uses two foveated renderers, with different values of the foveation parameter  $\sigma$ , for the dominant eye and the non-dominant eye, respectively. For the dominant eye, we choose the foveation parameter  $\sigma_d$  which results in an acceptable foveation level for both eyes. For the non-dominant eye, we choose  $\sigma_{nd} \geq \sigma_d$ , which corresponds to a higher foveation level. Because the non-dominant eye is weaker in sensitivity and acuity, the user is unable to notice the difference between the two foveation frames.

## 3.2 Eye-dominance-guided Foveated Rendering

Previous research on ocular dominance indicates that the non-dominant eye is weaker than the dominant eye in sensitivity and acuity. Here, we propose that the non-dominant eye is able to accept a higher level of foveation.

The overview of our eye-dominance-guided foveated rendering (EFR) system is shown in Fig. 2. In our EFR framework, for the baseline rendering, the system uses a KFR renderer with foveation parameter  $\sigma_d$  for the dominant eye and a KFR renderer with  $\sigma_{nd}$  for the non-dominant eye.

In the KFR algorithm, the parameter  $\sigma$  controls the width of the frame-buffer to be rendered, and the rendering time is proportional to the area of the rendered buffer. In other words, rendering time is inversely proportional to  $\sigma^2$ . Suppose the rendering time of the original frame for each eye is T, then the expected rendering time of KFR with  $\sigma_d = \sigma_{nd}$  is:

$$t_{FR} = \frac{T}{\sigma_d^2} + \frac{T}{\sigma_{nd}^2} = \frac{2T}{\sigma_d^2} \tag{6}$$

The expected rendering time of eye-dominance-guided foveated rendering (EFR) with  $\sigma_d \neq \sigma_{nd}$  is:

$$t_{EFR} = \frac{T}{\sigma_d^2} + \frac{T}{\sigma_{nd}^2} = \frac{T}{\sigma_d^2} \left( 1 + \left( \frac{\sigma_d}{\sigma_{nd}} \right)^2 \right) \tag{7}$$

Then,

$$\sigma_{d} \leq \sigma_{nd}$$

$$\Rightarrow \left(\frac{\sigma_{d}}{\sigma_{nd}}\right)^{2} \leq 1$$

$$\Rightarrow \frac{T}{\sigma_{d}^{2}} \left(1 + \left(\frac{\sigma_{d}}{\sigma_{nd}}\right)^{2}\right) \leq \frac{2T}{\sigma_{d}^{2}}$$

$$\Rightarrow t_{n} \leq t_{n} \leq t_{n}$$
(8)

Therefore, with  $\sigma_d \leq \sigma_{nd}$ , the rendering time for head-mounted displays can be reduced with non-perceivable difference between the foveated renderings for the dominant eye and the non-dominant eye.

The theoretical speedup *S* achieved by EFR is shown in Equation 9:

$$S = \frac{t_{FR}}{t_{EFR}} = \frac{2}{1 + \left(\frac{\sigma_d}{\sigma_{nd}}\right)^2} \ge 1. \tag{9}$$

Next, we conduct user studies to validate that the non-dominant eye is able to accept a higher level of foveation than the dominant eye, and also identify the foveation parameters for the dominant and non-dominant eyes.

## 4 USER STUDIES

We have conducted two user studies: a pilot study and a main study to identify the eye-dominance-guided foveated rendering parameters which can produce perceptually indistinguishable results compared with non-foveated rendering.

## 4.1 Apparatus

Our user study apparatus consists of an *Alienware* laptop with an NVIDIA GTX 1080 and a *FOVE* head-mounted display. The FOVE headset is integrated with a 120 Hz infrared eye-tracking system and a  $2560 \times 1440$  resolution screen ( $1280 \times 1440$  per eye). We use an *XBOX* controller for the interaction between the participant and the system. User studies took place in a quiet room.

As shown in Fig. 3, the computer-generated environments consist of 2 fireplace room scenes [22] and 8 scenes from the Amazon Lumberyard Bistro [20]. These scenes are rendered with the Unity game engine. To ensure that the participants are familiar with the user study system, we requested the participants to complete all the tasks for the trial run and familiarize themselves fully with the interaction before the formal tests.

## 4.2 Pre-experiment: Dominant Eye Identification

In both of the pilot study and the main study, we use the Miles Test [31] to measure the eye dominance for each participant before the start of the study.

First, the participant (TP) extends their arms out in front of themselves and creates a triangular opening between their thumbs and fore-fingers by placing their hands together at a 45-degree angle. Next, with both eyes open, TP centers the triangular opening on a goal object that is 20 feet away from TP. Then, TP closes their left eye with their right eye open. Finally, TP closes their right eye with their left eye open. If the goal object stays centered with the right eye open and is no longer framed by their hands with the left eye open, the right eye is their dominant eye. If the goal object stays centered with the right eye open, the left eye is their dominant eye. The Miles Test is performed twice for each participant, and we record TP's dominant eye and configure our renderer accordingly.

## 4.3 Pilot Study

We conduct a slider test and a random test in the pilot study. Each test consists of two steps:

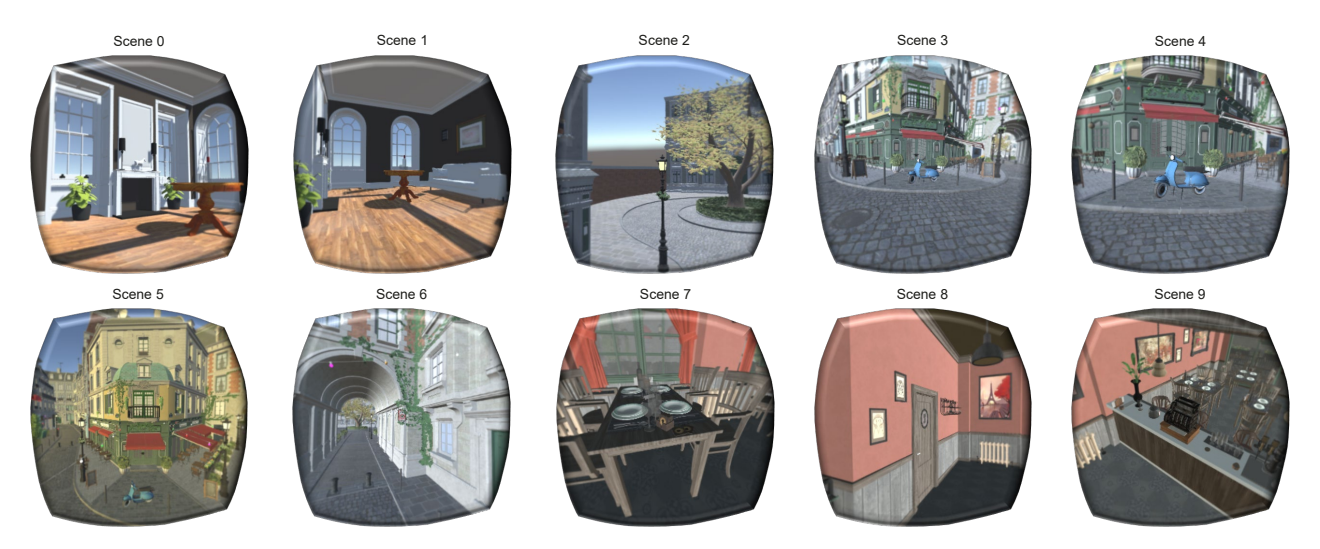


Fig. 3. The scenes used for the user study. Scene 0 and Scene 1 are animated *fireplace room* [22] and the other scenes are animated *Amazon Lumberyard Bistro* [20]. These scenes are rendered with the *Unity* game engine.

- 1. the participant estimates the *Uniform Foveation Parameter*  $\sigma_{UF}$  which is acceptable for both the dominant eye and the non-dominant eye. We express this condition as  $\sigma_d = \sigma_{nd} = \sigma_{UF}$ ;
- 2. the participant estimates the *Non-dominant Eye Foveation Parameter*  $\sigma_{NF}$  that results in the same overall visual perception as the uniform foveation, by increasing the foveation level (reducing overall detail) of the rendering for the non-dominant eye. We express this condition as:  $\sigma_d = \sigma_{UF}$ ,  $\sigma_{nd} = \sigma_{NF}$ .

## 4.3.1 Participants

We recruited 17 participants (5 females) at least 18 years old with normal or corrected-to-normal vision via campus email lists and flyers. The majority of participants had some experience with virtual reality. None of the participants was involved with this project prior to the user study.

The slider test allows the participants to navigate the foveation space

## 4.3.2 Slider Test

by themselves. We conduct the test with five different scenes with one trial for each scene. We present the two-step study protocol as follows. **1. Estimation of**  $\sigma_{UF}$ : In each trial, we first present the participant with the full-resolution rendering as a reference. Next, we present the participant with the same foveated rendering for both eyes and allow the participant to adjust the level of foveation by themselves: starting with the highest level of foveation,  $\sigma_d = 3.0$ , the participants progressively decrease the foveation level (with a step size of 0.2). The participants can switch between the foveated rendering result and the reference image back and forth until they arrive at the highest foveation level  $\sigma_{UF}$  (with the lowest overall level of detail) that is visually equivalent to the non-foveated reference.

**2. Estimation of**  $\sigma_{NF}$ : In each trial, we present the participant the foveated rendering with  $\sigma_d = \sigma_{UF}$  for the dominant eye, and allow the participant to adjust the level of foveation for the non-dominant eye. Starting with  $\sigma_{nd} = \sigma_{UF}$ , the participant can progressively increase the foveation level (with a step size of 0.2) until they reach the highest foveation level  $\sigma_{NF}$  that is perceptually equivalent to the foveated rendering with uniform foveation parameter  $\sigma_{UF}$ .

## 4.3.3 Random Test

The random test allows the participant to score the quality of the foveated rendering with different parameters in a random sequence. We conduct the test with five different scenes with one trial for each scene. The two steps are detailed below.

1. Estimation of  $\sigma_{UF}$ : In each trial, we present the participant with two frames: (1) the full-resolution rendering, and (2) the foveated rendering with  $\sigma_d = \sigma_{nd} = x$ , where x is selected from the shuffled  $\sigma$  parameter array with  $\sigma$  ranging between 1.2 and 3.0 with a step size of 0.2. The two frames are presented in a random order. We ask the participants to score the difference between the two frames they observe with unlimited time to make their decision. The score  $S_{UF}$  contains five confidence levels: 5 represents perceptually identical, 4 represents minimal perceptual difference, 3 represents acceptable perceptual difference, 2 represents noticeable perceptual difference, and 1 represents significant perceptual difference.

We use a pairwise comparison approach and the participants finish the trials with  $1.2 \le x \le 3.0$  in a random order. We choose the maximum x which results in an evaluation of *perceptually identical* or *minimal perceptual difference* with respect to the full-resolution (non-foveated) rendering, *i.e.*,

$$\sigma_{UF} = \underset{x}{\operatorname{argmax}} \ S_{UF}(x) \ge 4. \tag{10}$$

**2. Estimation of**  $\sigma_{NF}$ : In each trial, we present the participant with two frames: (1) foveated rendering with  $\sigma_d = \sigma_{nd} = \sigma_{UF}$ , and (2) foveated rendering with  $\sigma_d = \sigma_{UF}$ ,  $\sigma_{nd} = x$ , where x is selected from the shuffled parameter array with parameters ranging between  $\sigma_{UF}$  and 3.0 with a step size of 0.2. The two frames are presented in random order. We ask the participants to score the difference between the two frames they observed with unlimited time to make their decisions. The score  $S_{NF}$  contains five confidence levels: 5 represents perceptually identical, 4 represents minimal perceptual imbalance, 3 represents acceptable perceptual imbalance, 2 represents noticeable perceptual imbalance, and 1 represents significant perceptual imbalance.

We choose the maximum *x* that results in *perceptually identical* or *minimal perceptual imbalance* with respect to the uniform foveated rendering, *i.e.*,

$$\sigma_{NF} = \underset{x}{\operatorname{argmax}} \ S_{NF}(x) \ge 4. \tag{11}$$

## 4.3.4 Results and Limitations of the Pilot Study

From the pilot study, we find that: for most users, the dominant eye significantly dominates the visual perception and therefore eye-dominance-guided foveated rendering is likely to achieve significant speedup. We also observe that  $\sigma_{UF}$  and  $\sigma_{NF}$  do not correlate with the choice of scenes in a statistically significant manner. We provide the result and analysis of the pilot study in the supplementary material.

The pilot study yields a gap between the results of the slider test and the random test. We next present the potential reasons for this gap and our strategies for mitigating them:

- Performing a *single* trial for each test per scene is likely to induce some inaccuracy in parameter estimation. To mitigate this for the main study, we carry out *three* trials per scene per parameter;
- 2. In the pilot study, we use the maximum foveation parameter in Equations 10 and 11. We did this even if lower values of the foveation parameters led to an unacceptable score below 4. This was leading us to overestimate the foveation thresholds. In the main study, we use the greatest foveation parameter below which the user did not report an average score below 4. While this may reduce the speedups due to overall foveation, it will produce a higher perceptual quality;
- 3. We observe that  $\sigma_{NF}$  often reach our upper bound (3.0) 42.5% in the slider test and 60% in the random test. We have therefore increased the upper bound of  $\sigma_{NF}$  from 3.0 to 4.0 in the protocol of the main study;
- 4. In pilot study, we did not qualitatively evaluate the similarity in perceptual difference between EFR with the selected parameters and conventional foveated rendering (KFR) or regular rendering (RR). We therefore decide to add a quality evaluation in the main study.

Taking the above limitations and their mitigation strategies into account, we redesign the main study as described below.

## 4.4 Main Study

We conduct a slider test and a random test in the main study. There are three steps in both tests:

- 1. the participant estimates the *Uniform Foveation Parameter*  $\sigma_{UF}$ ;
- the participant estimates the Non-dominant Eye Foveation Parameter σ<sub>NF</sub>;
- 3. the participant qualitatively evaluates whether the EFR frames with  $\sigma_d = \sigma_{UF}$ ,  $\sigma_{nd} = \sigma_{NF}$  are perceptually the same with RR or traditional (non-dominant) KFR.

We use Scene 3, Scene 5, and Scene 6 in Fig. 3 for the parameter estimation in Steps 1 and 2 above. We use all the 10 scenes in Fig. 3 for the quality evaluation.

## 4.4.1 Participants

We recruited 11 participants (4 females) at least 18 years old with normal or corrected-to-normal vision via campus email lists and flyers. The majority of participants had some experience with virtual reality. None of the participants was involved with this project prior to the user study.

## 4.4.2 Slider Test

The slider test allows the participant to navigate the foveation quality space by themselves.

1. Estimation of  $\sigma_{UF}$ : We conduct the test on three scenes with three trials per scene. Therefore, there are 9 tests in total. For the n-th trial of scene m, we first present the participant with the full-resolution rendering, as a reference. Next, we present the participant with the same foveated rendering for both eyes and allow the participant to adjust the level of foveation by themselves: starting with the highest level of foveation,  $\sigma_d = 3.0$ , the participants progressively decrease the foveation level (with a step size of 0.2). The participant can switch between the foveated rendering result and the reference image back and forth until they can identify the lowest foveation level  $\sigma_{UF}(m,n)$  that is visually equivalent to the non-foveated reference. We calculate the mean uniform foveation parameter for scene m:

$$\sigma_{UF}(m) = \frac{1}{3} \sum_{n=1,2,3} \sigma_{UF}(m,n).$$
 (12)

We calculate the overall mean uniform foveation parameter:

$$\sigma_{UF} = \frac{1}{3} \sum_{m=1,2,3} \sigma_{UF}(m). \tag{13}$$

**2. Estimation of**  $\sigma_{NF}$ : We conduct the test on three scenes with three trials per scene. Therefore, there are 9 tests in total. For the *n*-th trial of scene *m*, we present the participant the foveated rendering with  $\sigma_d = \sigma_{UF}(m)$  for the dominant eye, and allow the participant to adjust the level of foveation for the non-dominant eye: starting with  $\sigma_{nd} = \sigma_{UF}(m)$ , the participants can progressively increase the foveation level (with a step size of 0.2) until they reach the highest foveation level  $\sigma_{NF}(m,n)$  that is perceptually equivalent to the foveated rendering with uniform foveation parameter  $\sigma_{UF}(m)$ .

Fig. 4 shows the change of parameters  $\sigma_{UF}$  and  $\sigma_{NF}$  in Step 1: Estimation of  $\sigma_{UF}$  and Step 2: Estimation of  $\sigma_{NF}$  in each trial.

Change of  $\sigma_{\text{UF}}$  and  $\sigma_{\text{NF}}$  in the Slider Test



Fig. 4. Change of parameter  $\sigma_d$  and  $\sigma_{nd}$  in the slider test. In Step 1, estimation of  $\sigma_{UF}$ , we present the participant with the same foveated rendering for both eyes and the participant progressively decrease the foveation level until  $\sigma_d = \sigma_{UF}(m)$ . In Step 2, estimation of  $\sigma_{NF}$ , we present the participant the foveated rendering with  $\sigma_d = \sigma_{UF}(m)$  for the dominant eye, and allow the participant to adjust the level of foveation for the non-dominant eye. The participant can progressively increase the foveation level until they reach the highest foveation level.

We calculate the mean uniform foveation parameter for scene m:

$$\sigma_{NF}(m) = \frac{1}{3} \sum_{n=1,2,3} \sigma_{NF}(m,n).$$
 (14)

We calculate the overall mean uniform foveation parameter:

$$\sigma_{NF} = \frac{1}{3} \sum_{m=1,2,3} \sigma_{NF}(m). \tag{15}$$

**3. Quality evaluation:** We conduct the A/B test on 10 scenes with 2 comparisons (EFR vs. KFR and EFR vs. RR) per scene, and 1 trial per scene per comparison. There are 20 trials in total. For scene m, we present the participant with two frames: (1) EFR with  $\sigma_d = \sigma_{UF}$ ,  $\sigma_{nd} = \sigma_{NF}$  and (2) RR or KFR with  $\sigma_d = \sigma_{nd} = \sigma_{UF}$ . The two frames are presented in random order. Then we ask the participants to score the difference between the two frames they observed with unlimited time to make their decisions. The score S(m) contains five confidence levels: 5 represents perceptually identical, 4 represents minimal perceptual difference, 3 represents acceptable perceptual difference, 2 represents noticeable perceptual difference, and 1 represents significant perceptual difference.

## 4.4.3 Random Test

The random test allows the participant to score the quality of foveated rendering with different parameters in a random sequence.

**1. Estimation of**  $\sigma_{UF}$ **:** We conduct the test on three scenes with 10 parameters per scene, each with three trials. Therefore, there are 90 tests in total. For the *n*-th trial of scene *m*, we present the participant

# συτ and σητ for the slider test and the random test 4.50 4.00 3.50 3.00 2.50 2.00 User 01 User 02 User 03 User 04 User 05 User 06 User 07 User 08 User 09 User 10 User 11 Slider σUF Random σUF Random σNF

Fig. 5. The average value of  $\sigma_{UF}$  and  $\sigma_{NF}$  in the slider test and the random test. A paired T-test reveals no significant difference (p = 0.8995 > 0.01) between the result of the slider test and the result of the random test.

with two frames: (1) the full-resolution rendering, and (2) the foveated rendering with  $\sigma_d = \sigma_{nd} = x$ , where x is selected from the shuffled parameter array with parameters ranging between 1.2 and 3.0 with a step size of 0.2. The two frames are presented in a random order. Then, we ask the participant to score the difference between the two frames they observed with unlimited time to make their decision. The score  $S_{UF}(m,n,x)$  contains five confidence levels: 5 represents perceptually identical, 4 represents minimal perceptual difference, 3 represents acceptable perceptual difference, 2 represents noticeable perceptual difference and 1 represents significant perceptual difference.

When the process is finished, we calculate the average score of all the trials for scene m with foveation parameter x:

$$S_{UF}(m,x) = \frac{1}{3} \sum_{n=1,2,3} S_{UF}(m,n,x).$$
 (16)

We choose the minimum x which results in an evaluation of *perceptually identical* or *minimal perceptual difference* with respect to the full-resolution (non-foveated) rendering as  $\sigma_{UF}(m)$ , i.e.,

$$\sigma_{UF}(m) = \underset{x}{\operatorname{argmin}} \ S_{UF}(m, x) \ge 4. \tag{17}$$

We calculate  $\sigma_{UF}$  using Equation 13.

**2. Estimation of \sigma\_{NF}:** We conduct the test on three scenes with Q parameters for scene m and three trials per scene per parameter. We compute Q using Equation 18 with  $\sigma_{max} = 4.0$  in the main study.

$$Q = \frac{\sigma_{max} - \sigma_{UF}(m)}{0.2} + 1 \tag{18}$$

For the *n*-th trial of scene *m*, we present the participant with two frames: (1) foveated rendering with  $\sigma_d = \sigma_{nd} = \sigma_{UF}(m)$ , and (2) foveated rendering with  $\sigma_d = \sigma_{UF}(m)$ ,  $\sigma_{nd} = x$ , where *x* is selected from the shuffled parameter array with *Q* parameters ranging between  $\sigma_{UF}(m)$  and  $\sigma_{max} = 4.0$  with a step size of 0.2. The two frames are presented in a random order. Then we ask the participants to score the difference between the two frames they observed with unlimited time to make their decisions. The score  $S_{NF}(m,n,x)$  contains five confidence levels: 5 represents *perceptually identical*, 4 represents *minimal perceptual imbalance*, 3 represents *acceptable perceptual imbalance*, 2 represents *noticeable perceptual imbalance* and 1 represents *significant perceptual imbalance*.

When the process is finished, we calculate the average score of all the trials for scene m with foveation parameter x:

$$S_{NF}(m,x) = \frac{1}{3} \sum_{n=1,2,3} S_{NF}(m,n,x).$$
 (19)

We choose the minimum x which results in an evaluation of *perceptually identical* or *minimal perceptual imbalance* with respect to the full-resolution (non-foveated) rendering as  $\sigma_{NF}(m)$ , i.e.,

$$\sigma_{NF}(m) = \underset{x}{\operatorname{argmin}} S_{NF}(m, x) \ge 4.$$
 (20)

We calculate  $\sigma_{NF}$  using Equation 15.

**3. Quality evaluation:** The quality evaluation is the same as that of the slider test.

## 4.5 Validity Test

## 4.5.1 Eye Tracking Data Analysis

We collected eye-tracking data from the FOVE HMD and would like to use it as a high-level validation to ensure that the participants are focusing at the desired fovea location.

However, we have noticed obvious tracking errors during the process: sometimes the eye-tracker fails to capture the movement of gaze and sometimes the tracked gaze position changes when the user blinks while focusing at the center of the screen. We also need to ensure that the users are paying attention to the user study instead of randomly choosing the answers. Therefore, it may not be ideal to solely depend on eye tracking results for judging the participants' focus. We also use the participant's performance with respect to the ground truth data to determine the accuracy and participant focus. We discuss this next.

## 4.5.2 Controlling for Lack of Attention and Exhaustion

We randomly inserted 30% of the trials to be validation trials in the random test to ensure the validity of the data in the pilot study and the main study. For uniform foveation parameter estimation, we presented the participants with identical full-resolution rendering results for both comparison frames as validation trials; for non-dominant eye foveation parameter estimation, we presented the participants with identical rendering results with  $\sigma_d = \sigma_{nd} = \sigma_{UF}$  for both comparison frames as validation trials. If the participant declared these validation trials to have a low score for similarity (3 or lower), we would ask the participant to pause and take a break for at least 30 seconds, and then continue the user study. Meanwhile, we would record this choice as an *error*. If  $error \ge 5$  in the random test, we would terminate the user study and discard the data of this participant. Based on this protocol, we discard one participant from the pilot study and mark the remaining 16 participants as valid data. All the 11 participants in the main study passed the validation trials.

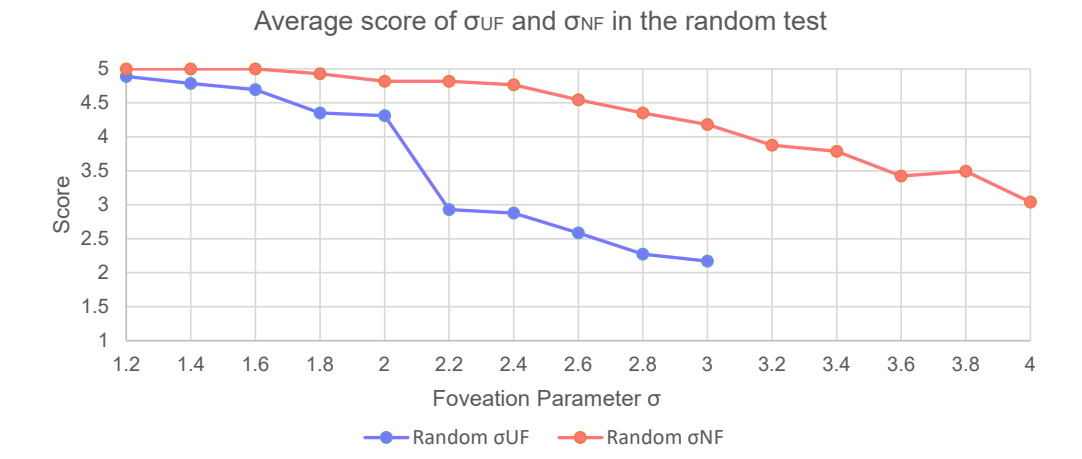


Fig. 6. The average score in Step 1 (Estimation of  $\sigma_{UF}$ ) and Step 2 (Estimation of  $\sigma_{NF}$ ) over different scenes and different users in the random test. To achieve *perceptually identical* and *minimal perceptual difference* between regular rendering and foveated rendering, we therefore choose  $\sigma_{UF} = 2.0$  and  $\sigma_{NF} = 3.0$  as our desired parameters.

Comparison	Score = 1	Score = 2	Score = 3	Score = 4	Score = 5
Slider: EFR vs. RR	0.00%	2.73%	8.18%	17.27%	71.82%
Slider: EFR vs. KFR	0.00%	4.55%	10.91%	30.00%	54.55%
Random: EFR vs. RR	0.00%	0.00%	0.91%	14.55%	84.55%
Random: EFR vs. KFR	0.00%	0.91%	3.64%	25.45%	70.00%

Table 1. The score frequency for different comparisons in the slider test and the random test. We notice that  $P(score \ge 4) \ge 85\%$  for both comparisons in the slider test and that  $P(score \ge 4) \ge 95\%$  for both comparisons in the random test. The result indicates the generalizability of eye-dominance-guided foveated rendering.

## 5 RESULTS AND ANALYSIS

In our main user study, the number of errors in the attention and exhaustion checking is less than 5 over all the participants. We use the results from all the 11 participants for data analysis.

## 5.1 Parameters Estimated with Different Scenes

We conducted a one-way ANOVA test [2,34] of the null hypothesis that the choice of scenes has no effect on the feedback of the participants. With the slider test, we did not find a significant effect of the choice of scenes on the feedback (with p = 0.9782 > 0.05).

## 5.2 Results of $\sigma_{UF}$ and $\sigma_{NF}$

For user i, we consider the averages of  $\sigma_{UF}$  (Equation 13) and  $\sigma_{NF}$  (Equation 15) over different scenes as the per-user foveation parameter for the dominant eye  $\sigma_{UF,i}$  and non-dominant eye  $\sigma_{NF,i}$ . We present these results in Fig. 5.

We first verified if there is a significant difference of the measured parameters ( $\sigma_{UF}$  and  $\sigma_{NF}$ ) between the slider test and the random test. With a paired T-test, we did not find a significant effect between the slider test and the random test (with p=0.8995>0.05). The paired T-test shows that the EFR parameters are stable with different experimental setups. We therefore take the average of slider test and the random test as the final parameters to test the rendering acceleration.

We further conducted statistical analysis on the difference between  $\sigma_{UF}$  and  $\sigma_{NF}$ . With a paired T-test, we found a significant effect that the foveation parameter  $\sigma_{UF}$  required for the non-dominant eye is higher than the foveation parameter  $\sigma_{NF}$  for the dominant eye (with  $p = 7.0530 \times 10^{-10} < 0.05$ ). Hence, we reach a conclusion that the disparity between the visual acuity in the dominant eye and the non-dominant eye is significantly different for the users.

For the random test, we also present the average score in Step 1 (estimation of  $\sigma_{UF}$ ) and Step 2 (estimation of  $\sigma_{NF}$ ) over different scenes and different users as shown in Fig. 6. We notice that both

 $S_{UF}$  and  $S_{NF}$  decrease with the increase of the foveation parameter. To achieve *perceptually identical* and *minimal perceptual difference* between regular rendering and foveated rendering for most users, we may choose  $\sigma_{UF} = 2.0$  and  $\sigma_{NF} = 3.0$  as the desired parameters.

## 5.3 Quality Evaluation

We analyzed whether there exists a significant difference of the quality evaluation results between the slider test and the random test. With the paired T-test, we did not find a significant effect between the slider test and the random test (with p = 0.8629 > 0.05).

We further verified if there exists a significant difference of the quality evaluation results between the experiment of EFR vs. KFR and the experiment of EFR vs RR. With a paired T-test, we found no significant difference between the result of the two experiments (with p = 0.9410 > 0.05).

The frequency from score = 1 to score = 5 is shown in Table 1. We notice that  $P(score \ge 4) \ge 85\%$  for both comparisons in the slider test and that  $P(score \ge 4) \ge 95\%$  for both comparisons in the random test. The result indicates the generalizability of eye-dominance-guided rendering. We can get acceptable perceptual quality that on different scenes with the measured parameters from the user study.

## 5.4 Rendering Acceleration

We have implemented the eye-dominance-guided foveated rendering pipeline in C++ 11 and OpenGL 4 on NVIDIA GTX 1080 to measure the rendering acceleration. We report our speedups based on the sophisticated Amazon Lumberyard Bistro dataset [20] at the resolution of  $1280 \times 1440$  per eye. The frame-rates and speedups of the original kernel foveated rendering (KFR) and the eye-dominance-guided foveated rendering (EFR) compared with traditional regular rendering (RR) are shown in Fig. 7. The speedup of the eye-dominance-guided foveated rendering compared with the original kernel foveated rendering ranges between  $1.06 \times$  and  $1.47 \times$  with an average speedup of  $1.35 \times$ .

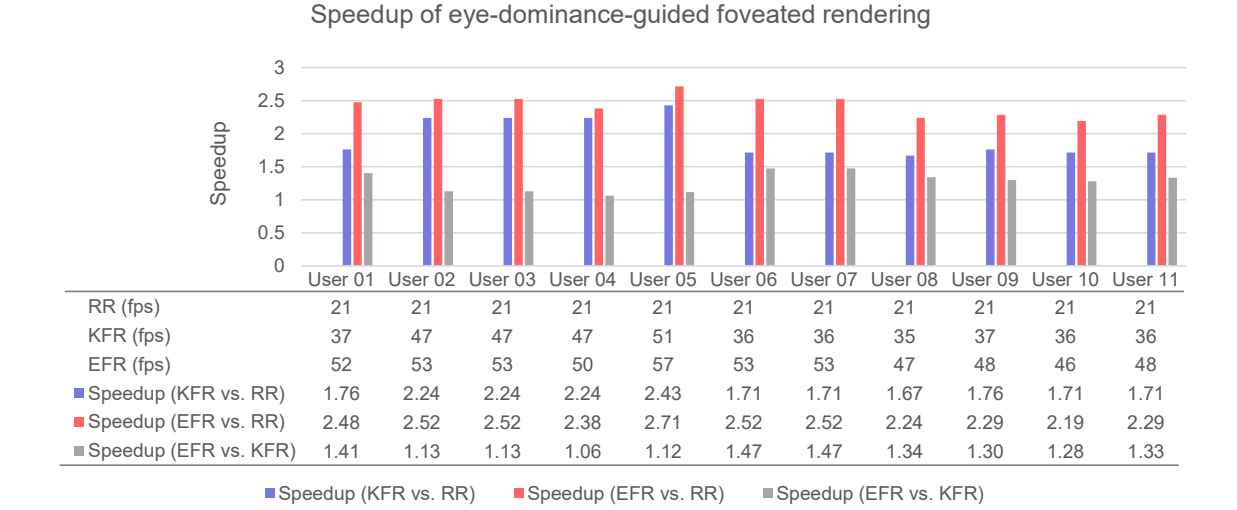


# Fig. 7. The measured frame-rates (in fps) and the speedups. The speedups of the eye-dominance-guided foveated rendering (EFR) compared with the original kernel foveated rendering (KFR) ranges between $1.06 \times$ and $1.47 \times$ with an average speedup of $1.35 \times$ . The speedups of EFR compared with regular rendering (RR) ranges between $2.19 \times$ and $2.71 \times$ with an average speedup of $2.38 \times$ .

## 6 CONCLUSIONS AND FUTURE WORK

In this paper, we have presented eye-dominance-guided foveated rendering (EFR), which achieves a significant speed-up by rendering the scene in the dominant eye with a lower foveation level (higher detail) and rendering the scene in the non-dominant eye with a higher foveation level (lower detail). This technique takes advantage of the ocular dominance property of the human visual system, and leverages the difference in acuity and sensitivity between the dominant eye and the non-dominant eye. Our approach can be easily integrated into the current rasterization rendering pipeline for head-mounted displays. We envision that EFR would be also beneficial to data streaming for networked VR applications such as Google Stadia<sup>1</sup>, Microsoft Project xCloud<sup>2</sup>, Montage4D [7], and Geollery [8] by reducing the bandwidth requirements.

## 6.1 Future Directions

## 6.1.1 Temporal Artifacts

One of the grand challenges in foveated rendering is handling artifacts due to temporal aliasing of moving objects [18], phase-aligned aliasing [38], and saliency-map based aliasing [36]. Since the eyedominance-guided foveated rendering relies on different levels of foveation for the two eyes, such challenges are likely to be even greater. We plan to study and address these challenges in the future work.

## 6.1.2 Personalized VR Rendering

Ocular dominance studies [4] indicate that 70% of the population is right-eye dominant and 29% is left-eye dominant. Thus, we expect that most users stand to benefit from eye-dominance-guided foveated rendering. In terms of personalized VR rendering, prior art has investigated how to personalize spatial audio for virtual environments using head-related transfer functions based on the ears' shape [44]. Further research may investigate how to enhance the visual experience of a user based on the eye prescription.

## 6.1.3 Further Leveraging Human Perception

An important argument in the study of visual direction is that there is a center or origin for judgments of visual direction called cyclopean

<sup>1</sup>Google Stadia: https://store.google.com/us/product/stadia

<sup>2</sup>Project xCloud: https://xbox.com/xbox-game-streaming/project-xcloud

eye [27]. Elbaum *et al.* [9] demonstrates that tracking accuracy is better with the cyclopean eye than with the dominant and non-dominant eye. Xia and Peli [42] propose a perceptual space model for virtual reality content based on the gaze point of the cyclopean eye. How the human visual system integrates the input from the two eyes into a cyclopean vision and how virtual reality in general, and foveated rendering in particular, could leverage it to improve visual quality and efficiency is deeply intriguing. We plan to delve into exploring how the foveated rendering system could be integrated with the cyclopean eye to further improve the immersive viewing experience and enhance the interaction accuracy between HMD and users.

## **ACKNOWLEDGEMENT**

We would like to thank the anonymous reviewers for the helpful comments that have significantly improved this paper. We also greatly appreciate the insightful suggestions by Dr. Eric Turner from Google. This work has been supported in part by the NSF Grants 14-29404, 15-64212, 18-23321, and the State of Maryland's MPower initiative. Any opinions, findings, conclusions, or recommendations expressed in this article are those of the authors and do not necessarily reflect the views of the research sponsors.

## REFERENCES

- [1] K. Bektas, A. Cöltekin, J. Krüger, and A. T. Duchowski. A Testbed Combining Visual Perception Models for Geographic Gaze Contingent Displays. In E. Bertini, J. Kennedy, and E. Puppo, eds., *Eurographics Conference on Visualization (EuroVis) - Short Papers*, pp. 67–71. The Eurographics Association, 2015. doi: 10.2312/eurovisshort.20151127
- [2] F. Buttussi and L. Chittaro. Locomotion in Place in Virtual Reality: A Comparative Evaluation of Joystick, Teleport, and Leaning. *IEEE Transactions on Visualization and Computer Graphics*, pp. 1–1, 2019. doi: 10.1109/TVCG.2019.2928304
- [3] R. Chaumillon, J. Blouin, and A. Guillaume. Eye dominance influences triggering action: The Poffenberger paradigm revisited. *Cortex*, 58:86 – 98, 2014. doi: 10.1016/j.cortex.2014.05.009
- [4] Chaurasia B.D. and Mathur B.B.L. Eyedness. Acta Anatomica, 96(2):301–305, 1976. doi: 10.1159/000144681
- [5] P. Clarberg, R. Toth, J. Hasselgren, J. Nilsson, and T. Akenine-Möller. AMFS: Adaptive Multi-Frequency Shading for Future Graphics Processors. ACM Trans. Graph, 33(4):141:1–141:12, 2014. doi: 10.1145/2601097.2601214

- [6] G. Denes, K. Maruszczyk, G. Ash, and R. K. Mantiuk. Temporal Resolution Multiplexing: Exploiting the limitations of spatio-temporal vision for more efficient VR rendering. *IEEE Transactions on Visualization and Computer Graphics*, 25(5):2072–2082, May 2019. doi: 10.1109/TVCG. 2019.2898741
- [7] R. Du, M. Chuang, W. Chang, H. Hoppe, and A. Varshney. Montage4D: Real-Time Seamless Fusion and Stylization of Multiview Video Textures. *Journal of Computer Graphics Techniques*, 1(15):1–34, Jan. 2019.
- [8] R. Du, D. Li, and A. Varshney. Geollery: A Mixed Reality Social Media Platform. In *Proceedings of the 2019 CHI Conference on Human Factors in Computing Systems*, p. 13. ACM, May 2019. doi: 10.1145/3290605. 3300915
- [9] T. Elbaum, M. Wagner, and A. Botzer. Cyclopean vs. dominant eye in gaze-interface-tracking. *Journal of Eye Movement Research*, 10(1), Jan. 2017. doi: 10.16910/jemr.10.1.2
- [10] S. Firdose, P. Lunqaro, and K. Tollmar. Demonstration of Gaze-Aware Video Streaming Solutions for Mobile VR. In 2018 IEEE Conference on Virtual Reality and 3D User Interfaces (VR), pp. 749–750, March 2018. doi: 10.1109/VR.2018.8447551
- [11] B. Guenter, M. Finch, S. Drucker, D. Tan, and J. Snyder. Foveated 3D Graphics. ACM Trans. Graph, 31(6):164:1–164:10, 2012. doi: 10.1145/ 2366145 2366183
- [12] Y. He, Y. Gu, and K. Fatahalian. Extending the Graphics Pipeline With Adaptive, Multi-Rate Shading. ACM Trans. Graph, 33(4):142:1–142:12, 2014. doi: 10.1145/2601097.2601105
- [13] H. Hoppe. Smooth View-Dependent Level-of-Detail Control and Its Application to Terrain Rendering. In *Proceedings of the Conference on Visualization* '98, VIS '98, pp. 35–42. IEEE Computer Society Press, Los Alamitos, CA, USA, 1998. doi: 10.1109/VISUAL.1998.745282
- [14] L. Hu, P. V. Sander, and H. Hoppe. Parallel View-Dependent Levelof-Detail Control. *IEEE Transactions on Visualization and Computer Graphics*, 16(5):718–728, Sept 2010. doi: 10.1109/TVCG.2009.101
- [15] A. Kaplanyan, A. Sochenov, T. Leimkühler, M. Okunev, T. Goodall, and G. Rufo. Deepfovea: Neural reconstruction for foveated rendering and video compression using learned natural video statistics. In ACM SIGGRAPH 2019 Talks, SIGGRAPH '19, pp. 58:1–58:2. ACM, New York, NY, USA, 2019. doi: 10.1145/3306307.3328186
- [16] J. Kim, Y. Jeong, M. Stengel, K. Akşit, R. Albert, B. Boudaoud, T. Greer, J. Kim, W. Lopes, Z. Majercik, P. Shirley, J. Spjut, M. McGuire, and D. Luebke. Foveated AR: Dynamically-foveated Augmented Reality Display. ACM Trans. Graph., 38(4):99:1–99:15, July 2019. doi: 10. 1145/3306346.3322987
- [17] B. Koçtekin, N. Ü. Gündoğan, A. G. K. Altıntaş, and A. C. Yazıcı. Relation of eye dominancy with color vision discrimination performance ability in normal subjects. *International journal of ophthalmology*, 6(5):733, 2013. doi: 10.3980/j.issn.2222-3959.2013.05.34
- [18] J. Korein and N. Badler. Temporal Anti-aliasing in Computer Generated Animation. In *Proceedings of the 10th Annual Conference on Computer Graphics and Interactive Techniques*, SIGGRAPH '83, pp. 377–388. ACM, New York, NY, USA, 1983. doi: 10.1145/800059.801168
- [19] P. Longhurst, K. Debattista, and A. Chalmers. A GPU Based Saliency Map for High-fidelity Selective Rendering. In *Proceedings of the 4th Inter*national Conference on Computer Graphics, Virtual Reality, Visualisation and Interaction in Africa, AFRIGRAPH '06, pp. 21–29. ACM, New York, NY, USA, 2006. doi: 10.1145/1108590.1108595
- [20] A. Lumberyard. Amazon lumberyard bistro, open research content archive (orca), July 2017. http://developer.nvidia.com/orca/amazon-lumberyard-bistro.
- [21] P. Lungaro, R. Sjöberg, A. J. F. Valero, A. Mittal, and K. Tollmar. Gaze-Aware Streaming Solutions for the Next Generation of Mobile VR Experiences. *IEEE Transactions on Visualization and Computer Graphics*, 24(4):1535–1544, April 2018. doi: 10.1109/TVCG.2018.2794119
- [22] M. McGuire. Computer graphics archive, July 2017. https://casual-effects.com/data.
- [23] I. McManus, C. Porac, M. Bryden, and R. Boucher. Eye-dominance, Writing Hand, and Throwing Hand. *Laterality: Asymmetries of Body, Brain and Cognition*, 4(2):173–192, 1 1999. doi: 10.1080/713754334
- [24] X. Meng, R. Du, M. Zwicker, and A. Varshney. Kernel Foveated Rendering. Proc. ACM Comput. Graph. Interact. Tech, 1(1):5:1–5:20, May 2018. doi: 10.1145/3203199
- [25] T. Ohshima, H. Yamamoto, and H. Tamura. Gaze-Directed Adaptive Rendering for Interacting With Virtual Space. In Proceedings of the 1996 Virtual Reality Annual International Symposium (VRAIS 96), VRAIS '96,

- pp. 103–110, 267. IEEE Computer Society, Washington, DC, USA, 1996. doi: 10.1109/VRAIS.1996.490517
- [26] A. Oishi, S. Tobimatsu, K. Arakawa, T. Taniwaki, and J. ichi Kira. Ocular dominancy in conjugate eye movements at reading distance. *Neuroscience Research*, 52(3):263 – 268, 2005. doi: 10.1016/j.neures.2005.03.013
- [27] H. Ono and R. Barbeito. The cyclopean eye vs. the sighting-dominant eye as the center of visual direction. *Perception & Psychophysics*, 32(3):201– 210, 1982. doi: 10.3758/BF03206224
- [28] A. Patney, M. Salvi, J. Kim, A. Kaplanyan, C. Wyman, N. Benty, D. Luebke, and A. Lefohn. Towards Foveated Rendering for Gaze-Tracked Virtual Reality. ACM Trans. Graph, 35(6):179:1–179:12, 2016. doi: 10.1145/2980179.2980246
- [29] C. Porac and S. Coren. The dominant eye. Psychological Bulletin, 83(5):880–897, 9 1976. doi: 10.1037/0033-2909.83.5.880
- [30] J. Ragan-Kelley, J. Lehtinen, J. Chen, M. Doggett, and F. Durand. Decoupled Sampling for Graphics Pipelines. ACM Trans. Graph, 30(3):17:1–17:17, 2011. doi: 10.1145/1966394.1966396
- [31] H. L. Roth, A. N. Lora, and K. M. Heilman. Effects of monocular viewing and eye dominance on spatial attention. *Brain*, 125(9):2023–2035, 09 2002. doi: 10.1093/brain/awf210
- [32] E. Shneor and S. Hochstein. Eye dominance effects in feature search. Vision Research, 46(25):4258 – 4269, 2006. doi: 10.1016/j.visres.2006. 08.006
- [33] M. Stengel, S. Grogorick, M. Eisemann, and M. Magnor. Adaptive Image-Space Sampling for Gaze-Contingent Real-Time Rendering. *Computer Graphics Forum*, 35(4):129–139, 2016. doi: 10.1111/cgf.12956
- [34] M. R. Stoline. The Status of Multiple Comparisons: Simultaneous Estimation of all Pairwise Comparisons in One-Way ANOVA Designs. *The American Statistician*, 35(3):134–141, 1981. doi: 10.1080/00031305.1981.10479331
- [35] Q. Sun, F.-C. Huang, J. Kim, L.-Y. Wei, D. Luebke, and A. Kaufman. Perceptually-guided Foveation for Light Field Displays. ACM Trans. Graph., 36(6):192:1–192:13, Nov. 2017. doi: 10.1145/3130800.3130807
- [36] M. Sung and S. Choi. Selective Anti-Aliasing for Virtual Reality Based on Saliency Map. In 2017 International Symposium on Ubiquitous Virtual Reality (ISUVR), pp. 16–19, June 2017. doi: 10.1109/ISUVR.2017.17
- [37] N. T. Swafford, J. A. Iglesias-Guitian, C. Koniaris, B. Moon, D. Cosker, and K. Mitchell. User, Metric, and Computational Evaluation of Foveated Rendering Methods. In *Proceedings of the ACM Symposium on Applied Perception*, SAP '16, pp. 7–14. ACM, New York, NY, USA, 2016. doi: 10. 1145/2931002.2931011
- [38] E. Turner, H. Jiang, D. Saint-Macary, and B. Bastani. Phase-Aligned Foveated Rendering for Virtual Reality Headsets. In 2018 IEEE Conference on Virtual Reality and 3D User Interfaces (VR), pp. 1–2. IEEE Computer Society, Los Alamitos, CA, USA, mar 2018. doi: 10.1109/VR. 2018.8446142
- [39] O. T. Tursun, E. Arabadzhiyska-Koleva, M. Wernikowski, R. Mantiuk, H.-P. Seidel, K. Myszkowski, and P. Didyk. Luminance-contrast-aware Foveated Rendering. ACM Trans. Graph., 38(4):98:1–98:14, July 2019. doi: 10.1145/3306346.3322985
- [40] K. Vaidyanathan, M. Salvi, R. Toth, T. Foley, T. Akenine-Möller, J. Nilsson, J. Munkberg, J. Hasselgren, M. Sugihara, P. Clarberg, T. Janczak, and A. Lefohn. Coarse Pixel Shading. In *Proceedings of High Performance Graphics*, HPG '14, pp. 9–18. Eurographics Association, Goslar Germany, Germany, 2014.
- [41] M. Weier, M. Stengel, T. Roth, P. Didyk, E. Eisemann, M. Eisemann, S. Grogorick, A. Hinkenjann, E. Kruijff, M. Magnor, K. Myszkowski, and P. Slusallek. Perception-Driven Accelerated Rendering. *Comput. Graph. Forum*, 36(2):611–643, 2017. doi: 10.1111/cgf.13150
- [42] Z. Xia and E. Peli. 30-1: Cyclopean eye based binocular orientation in virtual reality. SID Symposium Digest of Technical Papers, 49(1):381–384, 2018. doi: 10.1002/sdtp.12578
- [43] B. Yang, F. W. Li, X. Wang, M. Xu, X. Liang, Z. Jiang, and Y. Jiang. Visual Saliency Guided Textured Model Simplification. Vis. Comput., 32(11):1415–1432, Nov. 2016. doi: 10.1007/s00371-015-1129-4
- [44] D. Y. N. Zotkin, J. Hwang, R. Duraiswaini, and L. S. Davis. HRTF personalization using anthropometric measurements. In 2003 IEEE Workshop on Applications of Signal Processing to Audio and Acoustics (IEEE Cat. No.03TH8684), pp. 157–160, Oct 2003. doi: 10.1109/ASPAA.2003. 1285855